INFLUENCE OF THE SCATTERING POTENTIAL MODEL ON LOW ENERGY ELECTRON DIFFRACTION FROM Cu(001)–c(2 × 2)-Pb

W. HÖSLER and W. MORITZ

Institut für Kristallographie, Universität München, Theresienstrasse 41,
D-8000 Munich 2, Fed. Rep. of Germany

E. TAMURA

Institut für Festkörperphysik, Kernforschungsanlage Jülich, Postfach 1913,
D-5170 Jülich, Fed. Rep. of Germany

and

R. FEDER

Theoretische Festkörperphysik, FB 10, Universität Duisburg GH,
D-4100 Duisburg, Fed. Rep. of Germany

A dynamical LEED intensity analysis is reported for Cu(001)–c(2 × 2)-Pb. The adsorbate layer distance from the substrate is determined as 2.29 Å, and the topmost interlayer spacing for the substrate is the same as in bulk Cu, in contrast to a contraction for clean Cu(001). This structural result is, within the accuracy reached, insensitive to changes in the assumed scattering potential models. The *r*-factors suggest a weak preference for an energy-dependent exchange correlation and a moderate one for adding a localized adsorption part inside the muffin-tin spheres. The sensitivity of spectra and *r*-factors to changes in the assumed isotropic Debye temperature for Pb suggests that vibrational anisotropy should be taken into account in order to improve the accuracy of the analysis. Calculated spin polarization spectra are very sensitive to the exchange approximation, the localized absorption and the Debye temperature. Together with experimental data, they should be useful in particular for determining the vibrational anisotropy.

1. Introduction

The precision of surface structure analysis by comparing theoretical and experimental low-energy electron diffraction (LEED) spectra depends, from the theoretical side, on the adequacy of non-structural model ingredients and on the optimization of these ingredients within physically reasonable limits. The key quantity is the effective atomic scattering potential, particularly the exchange and correlation term. The influence of the atomic potential models on *I–V* profiles has been extensively studied for several clean surfaces [1–4] and some adsorption systems [5–8] and a clear preference for one of the

different approximations is still not yet given. For clean surfaces it is generally assumed that there is little influence of the potential model on the structural results, e.g. layer spacings, while for ionic adsorbates the situation is complicated by further parameters, such as the ionic radius and the charge transfer, which are unknown and have to be determined by fit to the experimental data.

For clean surfaces it has been found that the structure analysis can be improved including an energy dependence of the real part of the inner potential. The function $V_{0r}(E)$ can be obtained from experimental results by a fitting procedure [9–12] or directly by assigning certain peaks in the $I-V$ spectra to subthreshold effects which do not depend on the layer spacings in the surface region [13]. We adopt here a fitting procedure in which $V_{0r}(E)$ is represented by three independent variables. The resulting curve is very similar to the results obtained by Neve et al. [3] and Lindgren et al. [13] for the Cu(111) surface.

While the real part of the inner potential seems to be relatively well approximated and can be determined experimentally, the imaginary part, representing inelastic scattering effects, is far less understood. Usually, a uniform damping of the electron wave inside the crystal is assumed. On plain physical ground one would expect that this assumption is not sufficient and that a non-uniform damping model should improve the results. Recently, Lindgren et al. [13] introduced a model in which the interstitial region between the muffin-tin spheres was – for the optical potential – approximated by a stack of plates parallel to the surface. The interlayer attenuation is thus represented by two parameters and the result is that subthreshold peaks in the intensity spectra can be fitted to the experimental data. It has been shown, that non-uniform damping has an influence on $I-V$ spectra and may be responsible for some of the remaining discrepancies between theory and experiment.

We use here a different, physically more reasonable approach of a non-uniform damping model in which localized damping is assigned to the excitation of bound states in the muffin-tin spheres and which results in complex phase shifts δ_l above the corresponding thresholds. It has recently been shown that such a localized damping model has an important effect on spin polarization of LEED beams [14–16]. To calculate the polarization correctly the assumption of spin dependent localized damping parameters $\delta_l^{\pm}$ is necessary.

The purpose of this paper is to investigate different potential models and the influence of localized inelastic scattering on $I-V$ profiles and on spin polarization. We choose the metal overlayer system Cu(001)–c(2 × 2)-Pb, since for the clean Cu(001) surface excellent agreement between experimental and calculated curves has already been reached [4]. The less satisfactory result for the overlayer structure [17] has therefore to be assigned to scattering processes in the overlayer itself. Pb with its large electron density and strong scattering properties should be well suited to study the influence of different elastic and inelastic scattering models in detail. The agreement between theoretical and

experimental curves is good enough to determine the adsorption site. However, there remains some uncertainty in the Cu–Pb bond length.

We also investigate the spin polarization of diffracted beams, since it has been found that the spin polarization reacts often more sensitively to details of the potential than intensities. This is, in fact, quite practical for the structure analysis using the intensities, since here obviously the geometrical parameters are dominant. By spin polarization on the other hand, we can get clarity about the reliability of the approximation in the theory.

2. Experiments

The experiments were performed in a standard UHV chamber at pressures below 10^{-10} Torr. The chamber was equipped with the common facilities for alignment, sputtering, heating and cooling of the sample. The LEED optics were combined with a Faraday cup, movable by step motors on a hemisphere, surrounding the sample. The setting of energies, the movement of the Faraday cup and the acquisition of data were controlled by a minicomputer during all measurements. The experimental curves were obtained by normalizing the beam currents to the primary current, subtracting the background, determined in the vicinity of each beam, and by averaging the spectra of at least two symmetrically equivalent beams.

The copper sample was cleaned by series of argon ion sputtering and annealing, until no contaminations were detectable in the Auger spectra and all LEED beams had become sharp and brilliant. Intensity spectra of clean Cu(001) were measured and compared to calculated spectra, in order to check the condition of the surface and to test the data acquisition system. The agreement was comparable to the best results obtained for this surface [4], depicted by an averaged Zanazzi–Jona r-factor below 0.04.

Pb of high purity was evaporated from an rf-heated crucible. After bake-out of this source, the pressure rise during evaporation was below 10^{-11} Torr and no contaminations could be detected in the adsorbed layer. The coverage was adjusted by adsorption of more than the required half of a monolayer and by successive desorption of Pb during flashing the sample to about 700 K. The c(2 × 2) structure is only one of several sub-monolayer states of Pb on Cu(001) [17,18] and is very sensitive to slight changes of coverage. At a lower coverage additional beams of a c(4 × 4) structure became visible in the LEED pattern, and at higher coverages the half-order beams rapidly become diffuse and later on splitted into several satellites. In addition to a visual check of the LEED pattern, the quantitative evaluation of the Auger spectra was used to verify that all intensity spectra were taken at coverages, deviating not more than 2% of a monolayer from the optimum. The reproducibility of the coverages as determined from the peak to peak height of the Auger spectrum was 1%, while

the absolute coverage was determined taking the coverage of the optimum LEED pattern as 0.5.

The sample was cooled to about 160 K during all measurements, resulting in a considerable increase of contrast in both, LEED pattern and spectra.

3. Scattering potential models

We assume the potentials for both bulk and overlayer to have the muffin-tin form. The spherically symmetric charge densities $\rho(r)$ inside the muffin-tin spheres are obtained from free atom charge densities, which we calculate by the relativistic method of Liberman et al. [19], either by simple renormalization or by overlapping the contributions from atoms arranged in the fcc and c(2 × 2) configurations. In constructing the corresponding real ion core scattering potentials $V(r)$, we adopt the following local-density exchange-correlation approximations: (a) Xα with $\alpha = 0.7$ plus a relativistic exchange correlation as derived by MacDonald and Vosco [20], (b) the energy-dependent form suggested by Slater et al. [21], which corresponds to a local-density self-energy approximation in which the self-energy of the local homogeneous electron gas is treated in the Hartree–Fock approximation. Replacement of the latter by the random phase approximation, i.e. taking into account correlation effects, yields a complex potential, the real part $V_r^{HL}(E, r)$ of which has been given by Hedin and Lundquist [22] and successfully been employed in LEED calculations [1,3,5]. On the ground of results for spin polarization and differential cross section in electron scattering from Xe atoms [23] V_r^{HL} and V_r^{SWW} can be expected to produce LEED intensity spectra, which are very close to each other compared to spectra obtained from Xα potentials.

Inelastic scattering associated with the excitation of the localized 5d electrons of Pb gives rise (above the excitation threshold) to a nonuniform imaginary potential contribution, which – in a local self-energy approximation and in the muffin-tin model – may be written as $V_i(E, r)$, where E is the kinetic energy of the incident electrons. In view of the success of the local-density approximation for the real part $V_r(E, r)$, one might think of using a $V_i(E, r)$ obtained in the same way (e.g. by Hedin and Lundquist [22]). Since this procedure is based on a local homogeneous electron gas of density $\rho(r)$, it implies, however, not only the physically suspect concept of local plasmon excitation but also ascribes absorption power to core electrons below their excitation threshold. It is therefore not surprising that such $V_i(E, r)$ turned out a failure in electron–atom scattering (at energies below 100 eV) [24] and was wisely avoided in the LEED work of Neve et al. [5] and Lindgren et al. [13], who actually used Hedin and Lundquist's $V_r(E, r)$ but not their $V_i(E, r)$. Since a first-principles calculation of $V_i(E, r)$ involving the explicit use of the relevant 5d wave functions (e.g. along the lines of Ing and Pendry [25]) is
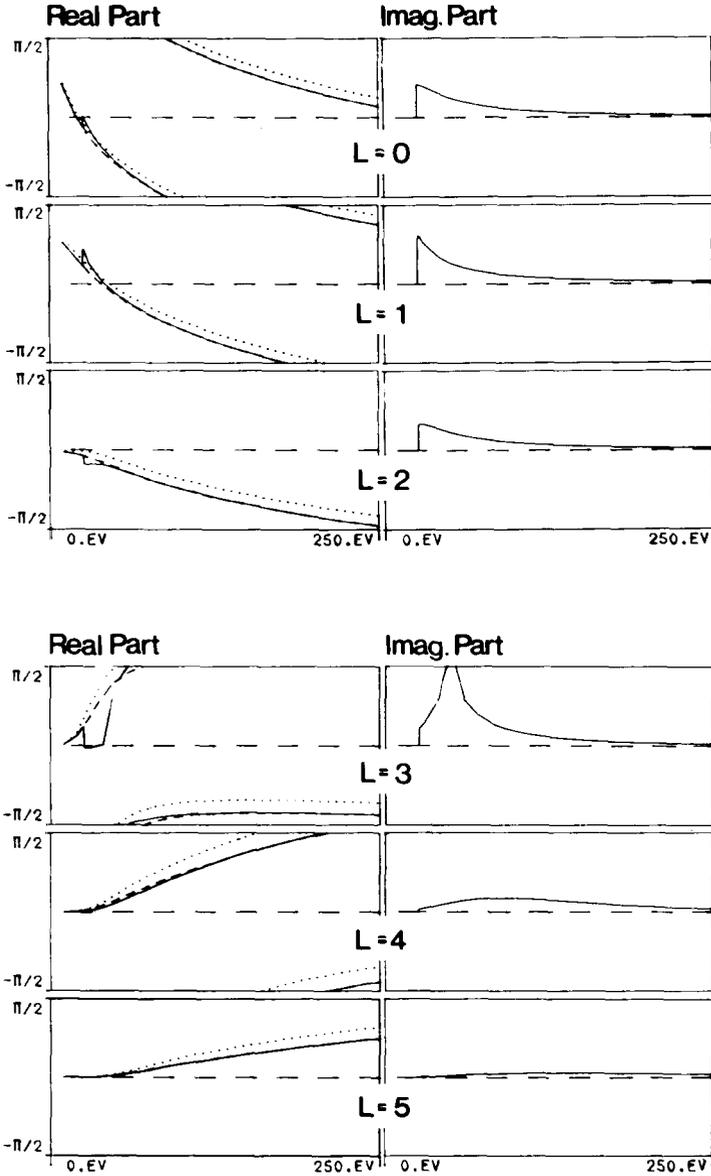
Fig. 1. The phase shifts of Pb used in the LEED calculations. Phase shifts derived for X α-exchange correlation (· · ·), for energy dependent exchange correlation (— — —) following Slater, Wilson and Wood, and for energy dependent correlation plus localized absorption, caused by excitation of the Pb 5d electrons, leading to complex phase shifts (———) are shown. Further details are given in the text.

complicated and presently not available, we employ a semi-phenomenological model, which was derived in the context of electron–atom scattering [26] and also used with success in spin-polarized LEED [14,16]:

$$V_i(E, r) = W(E) \, \rho_{5d}(r) \left[E - V_r(E, r) \right]^{-2},$$

where $\rho_{5d}(r)$ is the charge density of the 5d electrons; the "strength parameter" $W(E)$ is zero below the 5d excitation threshold and should, above the threshold, be adjusted such that the inelastic scattering cross section due to $(V_r + iV_i)$ reproduces experimental data. Since we are not aware of 5d inelastic cross section measurements for Pb, we "try out" several values for W, typically of the order of 6000 Ry^3 $bohr^3$ e_0^{-1}, which correspond to excitation cross sections of several $bohr^2$. We note that – in contrast to the abovementioned two-parameter slab-average V_i model of Lindgren et al. [13] – the present model firstly has the correct lattice periodicity and secondly explicitly employs the relevant partial charge density.

For the complex potential $V_r^{SWW}(E, r) + iV_i(E, r)$, the radial Dirac equation is solved numerically to yield complex partial wave scattering phase shifts $\delta_l^{\pm}(E)$. These phase shifts, labeled SWWLA (Slater–Wilson–Wood + local absorption) are shown in spin-averaged form $\delta_l = (\delta_l^+ + \delta_l^-)/2$ in fig. 1 together with the purely real ones, which originate from the real Xα and Slater–Wilson–Wood potential and are labeled Xα and SWW, respectively.

In all calculations where only uniform absorption was considered, the imaginary part of the optical potential was choosen, following previous LEED work, of the energy-dependent form $V_{0i} = 0.85(E + V_{0r})^{1/3}$. To ensure comparability of the results, the total absorption within the Pb layer was to remain unaffected by the localized absorption. In the calculations employing the inhomogeneous absorption, V_{0i} was reduced therefore by an amount $\tilde{V}_i$ corresponding to the spacial average of the inhomogeneous inelastic scattering cross section. $\tilde{V}_i$ can be expressed in terms of the imaginary part δ_{li} of the phase shifts as:

$$\tilde{V}_i = N(\pi/2) \left[2(E + V_{0r}) \right]^{-1/2} (2l + 1) \left[1 - \exp(-4\delta_{li}) \right],$$

where N is the number of atoms per unit volume (atomic units are used, with energies and potentials in hartrees). The real part of the inner potential V_{0r} was considered as an adjustable parameter, to be determined definitively in the course of the LEED spectra analysis.

4. Calculation of intensity and spin polarization

The ion core phase shifts $\delta_l^{\pm}$ are modified to incorporate isotropic lattice vibrations (cf. ref. [26], and references therein), assuming Debye temperatures

Θ_{Cu} of 330 K for Cu and Θ_{Pb} between 50 and 150 K for Pb. The resulting phase shifts are used in a relativistic multiple scattering formalism [27] to calculate spin polarization and intensity versus energy spectra for the optimal geometry of the adsorbate system. Since relativistic LEED calculations require about a factor of seven more computing time than their nonrelativistic counterparts, this geometry is determined by nonrelativistic LEED intensity calculations employing the spin-averaged phase shifts δ_l. The adequacy of this quasi-relativistic approximation was shown by Feder and Moritz [28] for Au ($Z = 81$) and is confirmed for Pb ($Z = 82$) by the present work. Up to 12 of these phase shifts were employed in the LEED intensity calculations which covered an energy range from 50 to 280 eV.

5. Intensity analysis

Preceding calculations gave evidence that the c(2 × 2) structure is formed by Pb atoms in the four-fold hollow sites of the Cu(001) surface [17]. The spacing of the adsorbate layer and a possible relaxation of the topmost substrate layer still bore some uncertainty and was treated here as variable geometric parameter.

A crucial parameter, entering the structure analysis, is the real part of the inner potential V_{0r}. Usually V_{0r} is assumed as constant and used as fitting parameter during comparison of the spectra. Since it shifts the peaks relative to the energy scale, as is also performed by a variation of the interatomic distances, V_{0r} strongly affects the resulting structural parameters. Here an energy dependent inner potential $V_{0r}(E)$ was derived in the course of a detailed r-factor analysis of the Cu(001) spectra by fitting the energy deviations of isolated peaks. A three parameter approach of the form $V_{0r}(E) = A + B(E + C)^{-1/2}$, with C fixed to about the Fermi energy plus the work function, reproduced the behaviour appropriately well. The energy dependence was derived separately for each of the assumed layer spacings by minimizing the energy deviations of isolated peaks and then was re-employed in a normal r-factor analysis for the respective model, thus enabling an independent fit of the energy dependence and the layer distance. For the SWW-exchange correlation spectra with and without local absorption an identical behaviour $V_{0r}^{SWW}(E)$ was found, with distinct deviations from the energy dependence $V_{0r}^{X\alpha}(E)$, which resulted from the Xα spectra. The optimum parameters for the energy dependence were $V_{0r}^{SWW}(E) = -3.9 - 57.8(E + 12.0)^{-1/2}$ eV and $V_{0r}^{X\alpha}(E) = -0.6 - 76.3(E + 12.0)^{-1/2}$ eV for the energy range between 40 and 280 eV. $V_{0r}^{SWW}(E)$ proved to be very similar to the inner potential V_{0r}^{HL}, which was calculated and confirmed for Cu(111) by Neve et al. [3] and Lindgren et al. [13] employing potential approaches of the Hedin and Lundquist form [22], – thus corroborating the abovementioned similarity of the HL and the SWW poten-

Table 1
R-factors for Cu(001)–c(2 × 2)-Pb

Beam		Θ_{Pb} (K)	$R(X\alpha)$	R(SWW)	R(SWWLA)
(0.5 0.5)		50	**0.285**	0.551	1.259
		70	0.316	0.358	0.929
		100	0.317	**0.168**	0.562
		150	0.361	0.221	**0.359**
(1 0)		50	0.107	0.122	0.126
		70	**0.101**	**0.095**	0.100
		100	0.164	0.132	**0.096**
		150	0.252	0.198	0.107
	(Cu(001)		0.058	0.046)	
(1 1)		50	**0.128**	**0.135**	0.119
		70	0.143	0.169	0.103
		100	0.154	0.201	**0.100**
		150	0.163	0.214	0.102
	(Cu(001)		0.034	0.034)	
(1.5 0.5)		50	**0.132**	0.154	0.163
		70	0.140	**0.124**	0.125
		100	0.197	0.149	**0.122**
		150	0.234	0.191	0.155
(1.5 1.5)		50	**0.037**	**0.026**	0.028
		70	0.045	0.032	**0.026**
		100	0.081	0.085	0.056
		150	0.142	0.167	0.113
(2 0)		50	0.097	0.089	0.083
		70	0.088	0.083	0.078
		100	**0.081**	**0.077**	0.071
		150	0.087	0.079	**0.067**
	(Cu(001)		0.075	0.045)	
(2 1)		50	0.124	0.092	0.093
		70	0.076	**0.066**	0.067
		100	**0.070**	**0.066**	**0.058**
		150	0.099	0.083	0.068
	(Cu(001)		0.039	0.034)	
Averaged		50	**0.112**	0.120	0.138
		70	**0.112**	**0.112**	0.110
		100	0.135	0.129	**0.100**
		150	0.168	0.163	0.112
	(Cu(001)		0.049	0.039)	

The dependency of the single-beam and the averaged Zanazzi–Jona *r*-factors on non-structural ingredients. Θ_{Pb} is the Debye temperature of Pb, and the two topmost layer spacings were $d_{Pb} = 2.30$ Å and $d_{Cu12} = 1.81$ Å for the model shown here. The *r*-factors of the clean Cu surface with respective layer spacings of $d_{Cu12} = 1.77$ Å and $d_{Cu23} = 1.83$ Å are given in parentheses. Minima of the *r*-factors are marked in bold.

tials. The energy dependence, originally determined for clean Cu(001), also was used for the c(2 × 2) adsorbate system and proved to be ideally suited with no need of further corrections.

The intensity spectra, obtained for the three potential models and various assumed spacings, were compared to the measured spectra by means of the r-factors defined by Pendry [29] and by Zanazzi and Jona [30], using the first 7 non-specular symmetrically inequivalent beams with a total energy range of 950 eV. Both r-factors lead to very similar results and for simplicity only the values of the latter one are given in table 1. In addition to the numerical r-factors, the visual comparison of the spectra was a complementary tool for testing the reliability.

For the clean Cu(001) surface the r-factors clearly demonstrate the superiority of the SWW approximation over the Xα approach. The r-factors of the c(2 × 2) adsorbate structure are however by a factor of 2 to 4 worse, compared to those obtained for the clean substrate, levelling off to a great extent the effects of the different potential approximations. Going from the Xα ($\alpha = 0.7$) exchange to the energy dependent (SWW) one, 6 of 7 individual-beam r-factors are seen to improve slightly, while one gets worse. A broad distribution of the optimal single-beam Debye temperatures of Pb is common to both models and levels down the weak preference in the r-factors, so that after averaging all beams the r-factors become the same for Xα and SWW. The overall impression from the visual comparison however retrieves a preference for the SWW exchange correlation (cf. fig. 2).

Localized absorption leads to a distinct decrease of the r-factors and some visible increase of accordance in the spectra. This improvement is accompanied by an increase of the appropriate Debye temperature Θ_{Pb}. The optimal value of Θ_{Pb} for the SWW spectra is about 70 K, rising to about 100 K when localized absorption is included. The correlation between localized absorption and optimal Θ_{Pb} holds on the average as depicted by the r-factors, but though local absorption and thermal vibrations enter the LEED calculations via the complex phase shifts, they differ in energy and angular momentum dependence, so that the effect of local absorption is not directly reproduced by an appropriate Debye temperature. Despite the mean correlation, the intensities thus are affected by both ingredients in a different and sometimes countercurrent manner (cf. e.g. the (1.5 0.5)-beam at 120 eV), so that the local absorption and a Θ_{Pb} of about 100 K prove to be necessary for a best accordance.

The r-factor analysis yields structural parameters which agree within 1% for the three potential approaches. The deviations, caused by the different scattering potentials, correspond to about half the standard deviation of this structure determination, roughly estimated from the distribution of the single-beam r-factor minima in parameter space. For the respective optimal values of Θ_{Pb} these deviations minimize for all three potential models to very similar values. The spacing of the adsorbate layer from the substrate was determined as
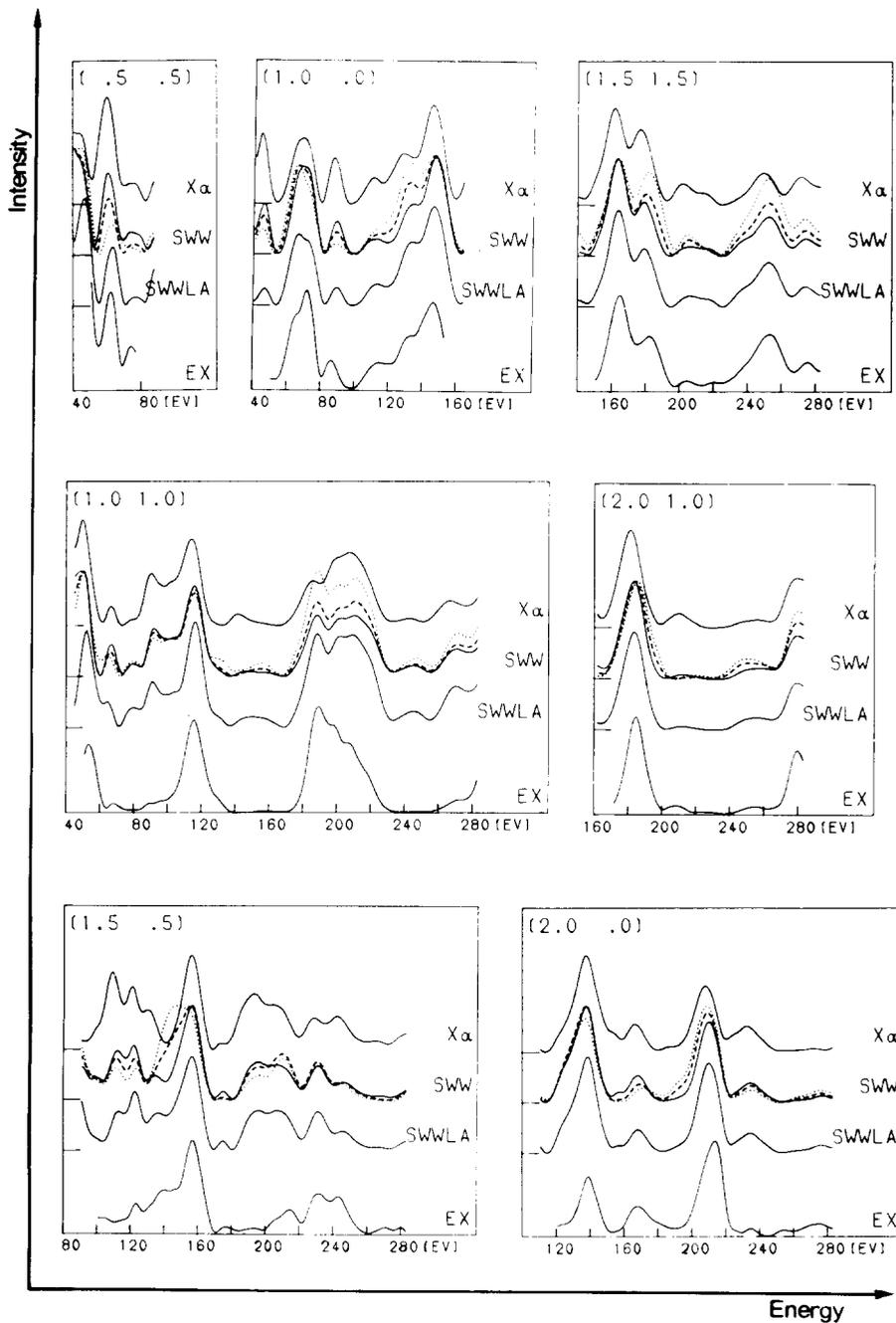
Fig. 2. Intensity spectra for Cu(001)–c(2×2)-Pb, calculated with the phase shifts from fig. 1 for adsorbate and topmost substrate layer spacings of 2.30 and 1.81 Å, respectively. The Pb Debye temperature Θ_{Pb} was 100 K for the full line spectra, and SWW spectra for additional Θ_{Pb} values of 50 K (· · ·) and 70 K (— — —) are also shown. For each beam the calculated intensities are given on the same (arbitrary) scale, whereas the experimental intensities were scaled up to fit the maxima.
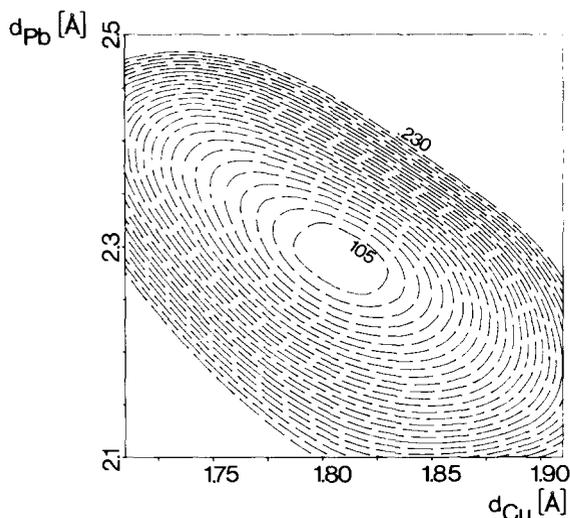
Fig. 3. Plot of the averaged Zanazzi–Jona r-factor against structural parameters. Results for the SWWLA approach and $\Theta_{Pb} = 100$ K are shown here.

2.29(4) Å (fig. 3), which is less than the value derived from the sum of both metallic radii (2.43 Å), indicating an about 4% closer Cu–Pb bond length. The topmost interlayer spacing in the substrate is 1.81(3) Å, identical to the bulk spacing and in contrast to the contraction which was found for the clean Cu(001) surface.

Though the energy dependent exchange correlation and the localized absorption improve the calculated spectra, this improvement is moderate, compared to the discrepancies of the spectra which remain unaffected by both ingredients. On the other hand the resulting structural parameters proved to be insensitive to these non-structural ingredients – thus corroborating the reliability of the common surface structure analysis with non-ideal potentials. It should be mentioned, however, that the sensitivity of the spectra to details of the scattering potential is in general higher in the lower energy range.

6. Spin polarization results

In fig. 4 we show spin polarization spectra, which were obtained by relativistic calculations using the geometrical structure determined by our intensity analysis. As one expects on the grounds of the atomic numbers of Cu ($Z = 29$) and Pb ($Z = 82$), the polarization values for the adsorbate system are, on the average, substantially larger (with maxima up to 60%) than for the clean substrate. The adsorbate system results for the Xα ($\alpha = 0.7$) and energy-depen-
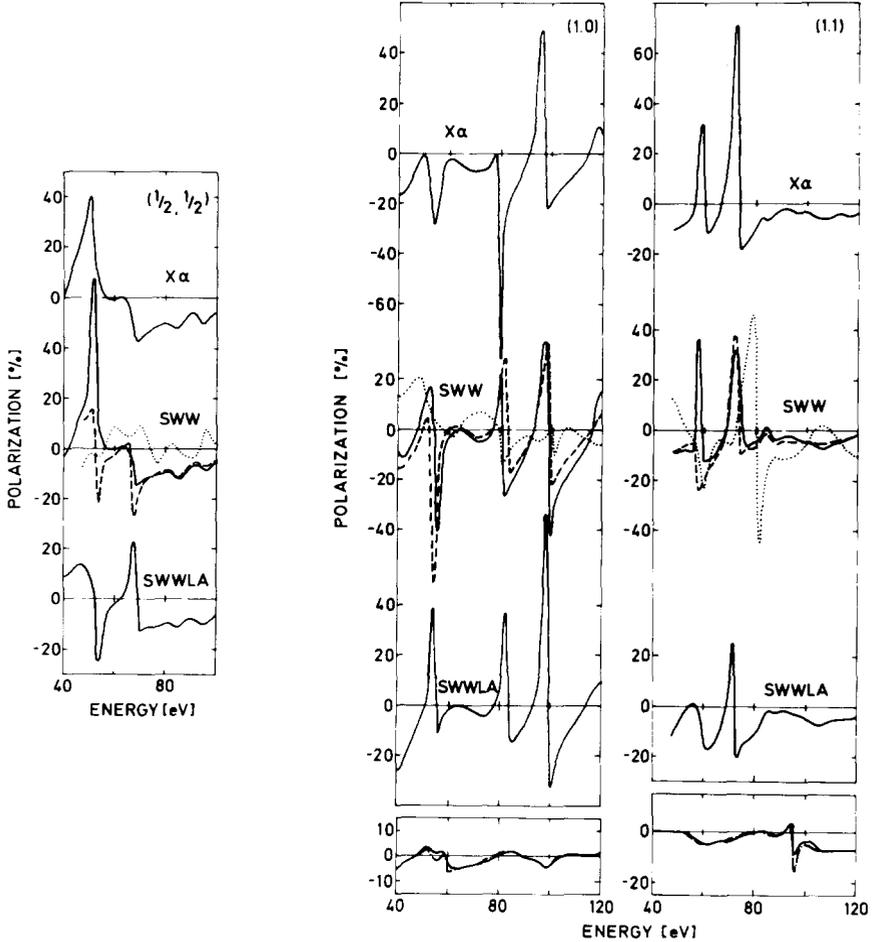
Fig. 4. Spin polarization spectra of Cu(001)–c(2×2)-Pb calculated for the intensity-derived geometry for beams and exchange potential approximations as indicated in the panels. The assumed Debye temperature of Pb was 100 K (——–), 70 K (— — —) and 50 K (· · ·). Separate bottom pannels for the integral-order beams: clean Cu(001) for SWW (——–) and Xα (α = 0.7) (· – · – ·) exchange.

dent (SWW) exchange approximations differ strongly in a number of features (e.g. in the (1 0) spectra near 50 and 80 eV). The same applies for the SWW spectra without and with localized absorption. The spectra for all beams and exchange approximations are, as illustrated in fig. 4 for three beams and the SWW exchange, also highly sensitive to a variation of the assumed Debye temperature Θ_{Pb}. With the exception of the (1 1) spectrum, lowering of Θ_{Pb} appears to reduce the overall spin polarization and smoothen the structure. This is plausible, since sharp structures originate generally from multiple

scattering, the amount of which decreases with decreasing Θ_{Pb}, i.e. increasing thermal lattice vibrations (in a single-scattering approximation, the polarization is that of a single muffin tin sphere and does not depend on the Debye temperature). Similar sensitivity (not shown here) was found with regard to changing the adsorbate–substrate spacing.

The above findings for the spin polarization from Cu(001)–c(2 × 2)-Pb are in accordance with results from other systems (cf. reviews in refs. [26,31,32] and references therein) and corroborate the idea that spin polarization (or, equivalently, the intensity asymmetry obtained by means of a polarized-electron gun) permits, via comparison between theory and experiment, a refinement in the determination of structural and non-structural parameters by LEED.

7. Conclusions

The energy-dependent exchange correlation approach noticeably improves the calculated spectra of clean Cu(001). For the Cu(001)–c(2 × 2)-Pb adsorbate system there is only a weak preference for the energy-dependent exchange and a moderate superiority of the localized-absorption approach. Both effects can neither explain nor eliminate the remaining discrepancies between experimental and calculated intensities, necessitating another approach to improve the accordance of the spectra and thereby the accuracy of the analysis. Experimental errors, such as small changes in the coverage or deviations from normal incidence, can be ruled out as a possible source for the remaining discrepancies. It has been proved experimentally that small changes in the coverage produce very little changes in the $I–V$ spectra and the normal incidence was checked carefully. Both spectra and r-factors are considerably sensitive to the Debye temperature of the adsorbate, with remaining uncertainties depicted by the broad distribution of the optimal single-beam values. A general defect, however, of the common LEED calculations are the employed isotropic lattice vibrations, since the atoms of influence and interest – the surface atoms – are far from an isotropic surrounding. The anisotropic thermal effects are additionally enhanced in a layer of low Debye temperature material that is condensed on a substrate of a high one, as it holds for Pb on Cu. We therefore attribute as the most probable source for the residual experiment–theory misfit the employed isotropic Debye temperature of Pb and we suppose that by anisotropic lattice vibrations, especially for the adsorbate, the accuracy of surface structure analysis can be improved in the same manner as it was possible for X-ray analysis some decades ago. Alternative sources of the discrepancies are, of course, the muffin-tin approximation on which all LEED calculations are based and the use of nonselfconsistent scattering potentials. The influence of non-spherical potentials is not yet known but is possibly of similar importance as anisotropic temperature factors. The use of selfconsistent

potentials seems to be of minor importance because the different model tested here showed little influence on the spectra. The sensitivity of the calculated spin polarization to the potential approximations and in particular to the Debye temperature suggests that comparison of experimental and theoretical spin polarization spectra should be valuable also for determining anisotropic lattice vibrations effects.

References

[1] P.M. Echenique and D.J. Titterinton, J. Phys. C10 (1977) 625.
[2] H.B. Nielsen and D.L. Adams, J. Phys. C15 (1982) 615.
[3] J. Neve, P. Westrin and J. Rundgren, J. Phys. C16 (1983) 1291.
[4] H.L. Davis and J.R. Noonan, in: Surface Structure Determination by LEED, Eds. P.M. Marcus and F. Jona (Plenum, New York, 1984);
  H.L. Davis and J.R. Noonan, J. Vacuum Sci. Technol. 20 (1982) 842; Surface Sci. 126 (1983) 245.
[5] J. Neve, J. Rundgren and P. Westrin, J. Phys. C15 (1982) 4391.
[6] S.A. Lindgren, L. Walldén, J. Rundgren, P. Westrin and J. Neve, Phys. Rev. B28 (1983) 6707.
[7] A. Salwén and J. Rundgren, Surface Sci. 53 (1975) 523.
[8] S.Y. Tong, A. Maldonaldo, C.H. Li and M.A. Van Hove, Surface Sci. 94 (1980) 73.
[9] J.E. Demuth, P.M. Marcus and D.W. Jepsen, Phys. Rev. B11 (1973) 1460.
[10] P.J. Jennings and S.M. Thurgate, Surface Sci. 104 (1981) L210.
[11] S. Hengrasmee, K.A.R. Mitchell, P.R. Watson and S.J. White, Can. J. Phys. 58 (1980) 200.
[12] Y. Gauthier, R. Baudoing and C. Clarke, J. Phys. C15 (1982) 3231.
[13] S.A. Lindgren, L. Walldén, J. Rundgren and P. Westrin, Phys. Rev. Letters 50 (1983) 368; Phys. Rev. B29 (1984) 576.
[14] E. Tamura and R. Feder, Solid State Commun. 44 (1982) 1101; Vacuum 33 (1983) 864.
[15] R. Feder, S.F. Alvarado, E. Tamura and E. Kisker, Surface Sci. 127 (1983) 83.
[16] R. Feder and J. Kirschner, Surface Sci. 103 (1981) 75.
[17] W. Hösler, Thesis, Universität München (1982);
  W. Hösler and W. Moritz, Surface Sci. 117 (1982) 196.
[18] J. Henrion and G.E. Read, Surface Sci. 29 (1972) 20.
[19] D. Liberman, J.T. Weber and D.T. Cromer, Phys. Rev. 137 (1965) A27.
[20] A.H. MacDonald and S.H. Vosco, J. Phys. C12 (1979) 2977.
[21] J.C. Slater, T.M. Wilson and J.H. Wood, Phys. Rev. 179 (1969) 28.
[22] B.F. Lundquist, Phys. Status Solidi 32 (1968) 273;
  L. Hedin and B.F. Lundquist, J. Phys. C4 (1971) 2064.
[23] B. Awe, F. Kemper, F. Rosicky and R. Feder, J. Phys. B16 (1983) 603.
[24] M.S. Woolfson, S.J. Gurman and B.W. Holland, Surface Sci. 117 (1982) 450.
[25] B.S. Ing and J.B. Pendry, J. Phys. C8 (1975) 1087.
[26] J.B. Furness and I.E. McCarthy, J. Phys. B6 (1973) 2280;
  C.B. Lucas and I.E. McCarthy, J. Phys. B11 (1978) L301, and references therein.
[27] R. Feder, J. Phys. C14 (1981) 2049.
[28] R. Feder and W. Moritz, Surface Sci. 77 (1978) 505.
[29] J.B. Pendry, J. Phys. C4 (1971) 3095.
[30] E. Zanazzi and F. Jona, Surface Sci. 62 (1977) 61.
[31] R. Feder, in: Surface Structure Determination by LEED, Eds. P.M. Marcus and F. Jona (Plenum, New York, 1984).
[32] F.B. Dunning and G.K. Walters, in: Polarized Electrons in Surface Physics, Ed. R. Feder (World Scientific, Singapore, 1985).